

# The Conversion of Nanocellulose into Solvent-free Nanoscale Liquid crystals by Attaching Long Side-arms for Multi-responsive Optical Materials

*Qiaoyun Cheng,<sup>a</sup> Pan Chen,<sup>c</sup> Dongdong Ye,<sup>a</sup> Junmei Wang,<sup>a</sup> Guangjie Song,<sup>d</sup> Junjie Liu,<sup>e</sup> Zhiquan Chen,<sup>e</sup> Lingyun Chen,<sup>f</sup> Qi Zhou,<sup>\*bc</sup> Chunyu Chang,<sup>\*a</sup> and Lina Zhang<sup>\*a</sup>*

<sup>a</sup> College of Chemistry and Molecular Sciences, Hubei Engineering Center of Natural Polymer-based Medical Materials, Wuhan University, Wuhan 430072, China

<sup>b</sup> Division of Glycoscience, Department of Chemistry, KTH Royal Institute of Technology, AlbaNova University Centre, SE-106 91 Stockholm, Sweden

<sup>c</sup> Wallenberg Wood Science Center, Department of Fiber and Polymer Technology, KTH Royal Institute of Technology, SE-100 44 Stockholm, Sweden

<sup>d</sup> CAS Key Laboratory of Engineering Plastics, CAS Research/Education Center for Excellence in Molecular Sciences, Institute of Chemistry, Chinese Academy of Sciences, Beijing 100190, China

<sup>e</sup> Hubei Nuclear Solid Physics Key Laboratory, Department of Physics, Wuhan University, Wuhan 430072, China

<sup>f</sup> Department of Agricultural, Food and Nutritional Science, University of Alberta, Edmonton, AB, T6G 2P5, Canada.

## **Molecular dynamics simulations details**

**Model construction:** The model contains 13 layers on 10 plane, 23 layers on 110 plane, and 27 layers of chains along 200 plane. This corresponds to the size in cross-section of  $\sim 8$ ,  $\sim 12$  and  $\sim 11$  nm that estimated from the wide angle X-ray diffraction data. Each glucan chain within the fibril contained DP 8 and covalently linked to its periodic image along the chain direction while applying periodic boundary condition. Since glucan chain in native cellulose fibril is at least 150 nm long and usually has DP more than 300, for which the current computational power can hardly handle when using fully atomistic dynamics simulation, this strategy is commonly applied to simulate the infinite chains and is the “only” way to mimic a cellulose chain that is long enough at atomistic scale precision over several nanoseconds of timescale.<sup>1</sup> The energetically more stable hydrogen bonding pattern A was selected.<sup>2</sup>

The exposed hydroxyl groups on exterior surface chain were “in silico chemically”, selectively modified to be grafted with DC5700. The exterior O2, O3, O6 from all the exposed hydroxyl groups, beside those on 200 plane, are modified. This corresponds to a fully substitution of accessible surface. The NPES chain was placed initially with the charged end group toward cellulose surface. The system was initially centered in the simulation box with dimension of  $40 \times 40 \times 4.152$  nm<sup>3</sup>.

**Force field:** Molecular dynamics simulations were performed using GROMACS package, version 2018.3. The CHARMM general force field<sup>3-4</sup> was used to

describe DC5700 and NPES. The CHARMM36 carbohydrate force field<sup>5-6</sup> was used for cellulose.

**Set up:** The initial structures were optimized by energy minimization using the standard methods named steepest descents and conjugate gradient. A short equilibration of 1 ns was performed using NVT ensemble (constant number of particle, volume and temperature). The system was followed by a production run of 4 ns with a time step of 2 fs using NPT ensemble (constant number of particle, pressure and temperature). Temperature was controlled at 300 K using velocity-rescaling algorithm<sup>7</sup> and the pressure was regulated at 1 Bar using Berendsen algorithm.<sup>8</sup> The cutoff of 1.0 nm was used for short range non-bonded interaction (the electrostatic and Lennard-Jones interaction). Dispersion and pressure in long range was corrected. The long range electrostatic interaction was calculated using particle mesh method summation.<sup>9</sup> Periodic boundary condition (PBC) was applied in all three directions. The trajectory files in production lasted for 100 ns in total and were saved every 20 ps.

## Grafting density of the canopy

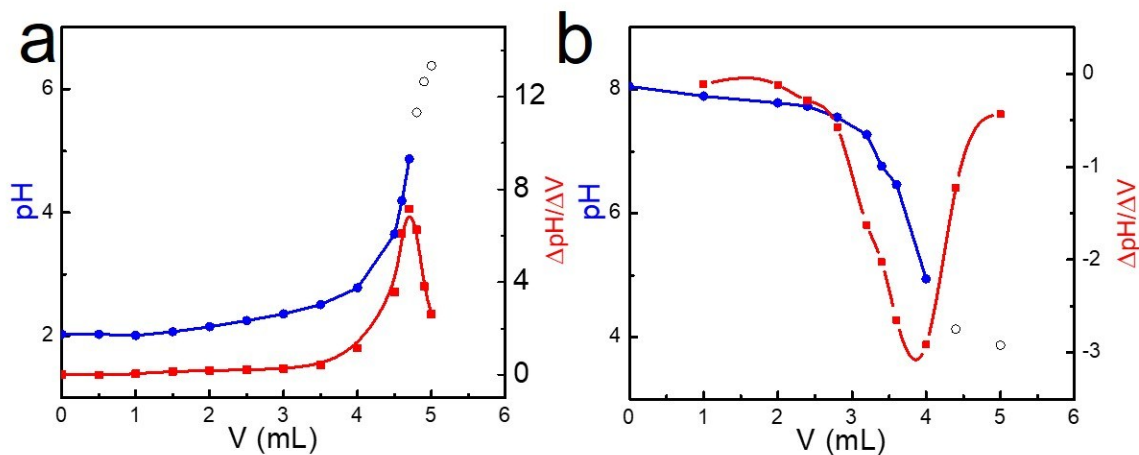


**Fig. S1.** Titration curves of nanoliquids of TCNC-*g*-SiSO<sub>3</sub>H-AC1815 (a) and TCNC-*g*-DC5700-NPES (b).

AC1815 (0.1 g/mL) was dropped into 10 g 2 wt% TCNC-*g*-SiSO<sub>3</sub>H aqueous dispersion. When reached equivalence was reached, 4.8 mL AC1815 (0.1 g/mL) was added and the pH value was 5.68. For fabricate TCNC-*g*-DC5700-NPES, 6 g 3 wt% TCNC-*g*-DC5700 aqueous dispersion was titrated with 0.06 g/mL NPES, the pH value was decreased to 4.94 when 4mL NPES solution was added at equivalence point.

According to the bulk degree of substitution ( $DS_b$ ) could be calculated from molar mass of grafted moiety ( $M_g$ ) and content of grafted moiety ( $C_g$ ) according to the titration curves:

$$DS_b = \frac{162C_g}{C_{TCNC}M_g}$$

Based on the cross-sections of TCNCs deduced from the analysis of WAXS curve shown in Figure 2a, there are a total of 259 chains and 60 surface chains in TCNC. The conversion relations between  $DS_b$  and surface degree of substitution ( $DS_s$ ) :

$$DS_s = \frac{259}{60} DS_b$$

**Table S1.** Grafting density of canopy on TCNCs.

Nanofluids	Grafted moiety	Molar mass of grafted moiety ( $M_g$ )	Content of grafted moiety ( $C_g$ )	$DS_b$	$DS_s$
TCNC-g-SiSO <sub>3</sub> H-AC1815	AC1815	~1589	70.1%	0.24	1.04
TCNC-g-DC5700-NPES	DC5700-NPES	~1180	82.4%	0.64	2.76

The  $DS_b$  also could be measured from the sulfur element ( $C_S$ ) and nitrogen element content ( $C_N$ ) for TCNC-g-SiSO<sub>3</sub>Na and TCNC-g-DC5700, respectively:

$$C_S = \frac{32DS_b(S)}{162 + 206DS_b(S)}$$

$$C_N = \frac{14DS_b(N)}{162 + 402DS_b(N)}$$

**Table S2.** Elemental analysis data for TCNC-g-SiSO<sub>3</sub>H and TCNC-g-DC5700.

Sample	C%	H%	N%	S%	$DS_b$	$DS_s$	/ : The cont ent was belo w
TCNC-g-SiSO <sub>3</sub> H	41.600	6.210	/	1.280	0.07	0.30	
TCNC-g-DC5700	53.050	9.368	2.069	/	0.58	2.50	

the detection limit.

## Crystallite size

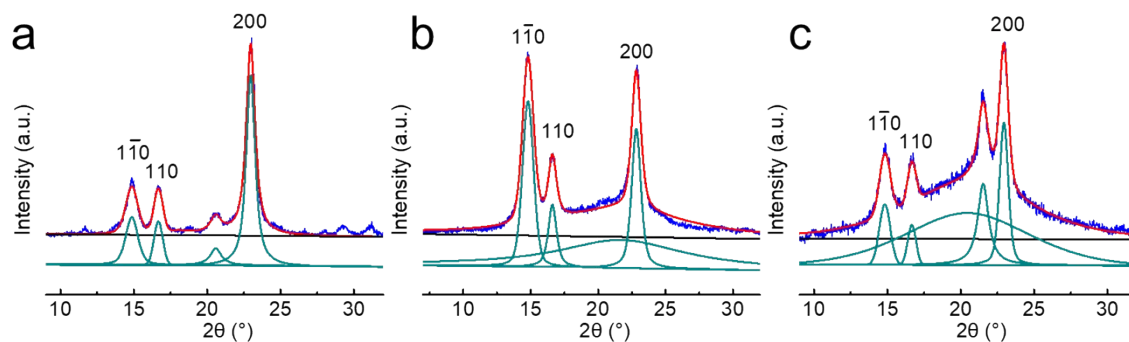


**Fig. S2.** The WAXS curves of TCNCs (a), TCNC-g-SiSO<sub>3</sub>Na (b), TCNC-g-DC5700 (c).

**Table S3.** TCNCs, TCNC-g-SiSO<sub>3</sub>Na, TCNC-g-DC5700 crystallite width estimated from WAXS curves.

Peak	TCNCs (nm)	TCNC-g-SiSO <sub>3</sub> Na (nm)	TCNC-g-DC5700 (nm)
10	8.2	8.2	9.1
110	11.4	11.1	12.1
200	11.1	10	11.5

## FTIR analysis

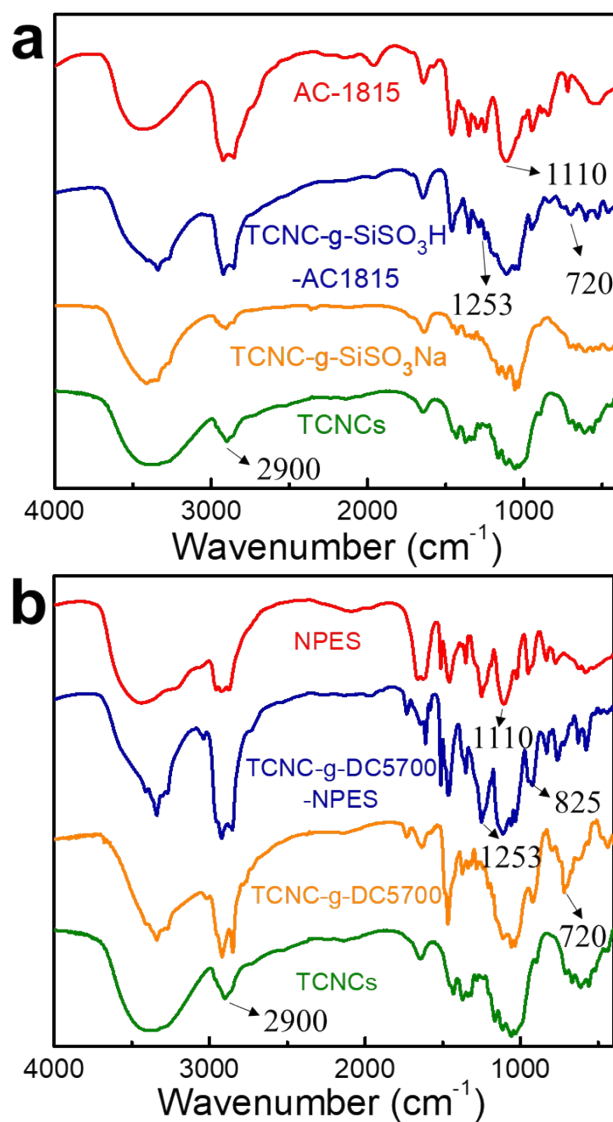


**Fig. S3.** FTIR spectra of TCNCs, TCNC-g-SiSO<sub>3</sub>Na, TCNC-g-SiSO<sub>3</sub>H-AC1815, AC1815 (a), and TCNCs, TCNC-g-DC5700, TCNC-g-DC5700-NPES and NPES (b).

The new peak at 720  $\text{cm}^{-1}$  was ascribed to C-H bending vibration of the long alkane chain in TCNC-g-DC5700. The incorporation of AC1815 counter-ion was successful as the new peaks at 720  $\text{cm}^{-1}$  and 1110  $\text{cm}^{-1}$  were observed in the TCNC-g-SiSO<sub>3</sub>H-AC1815 sample for the octadecyl group and the C-O-C stretching vibration of PEG chain, respectively. For the TCNC-g-DC5700-NPES sample, the absorption band of  $\text{SO}_3^-$  appeared at 1253  $\text{cm}^{-1}$ , and the stretching vibration of C-O-C and phenyl group

were observed at  $1110\text{ cm}^{-1}$  and  $825\text{ cm}^{-1}$ , respectively, indicating the electrostatic binding of counter-ion NPES.

### XPS analysis

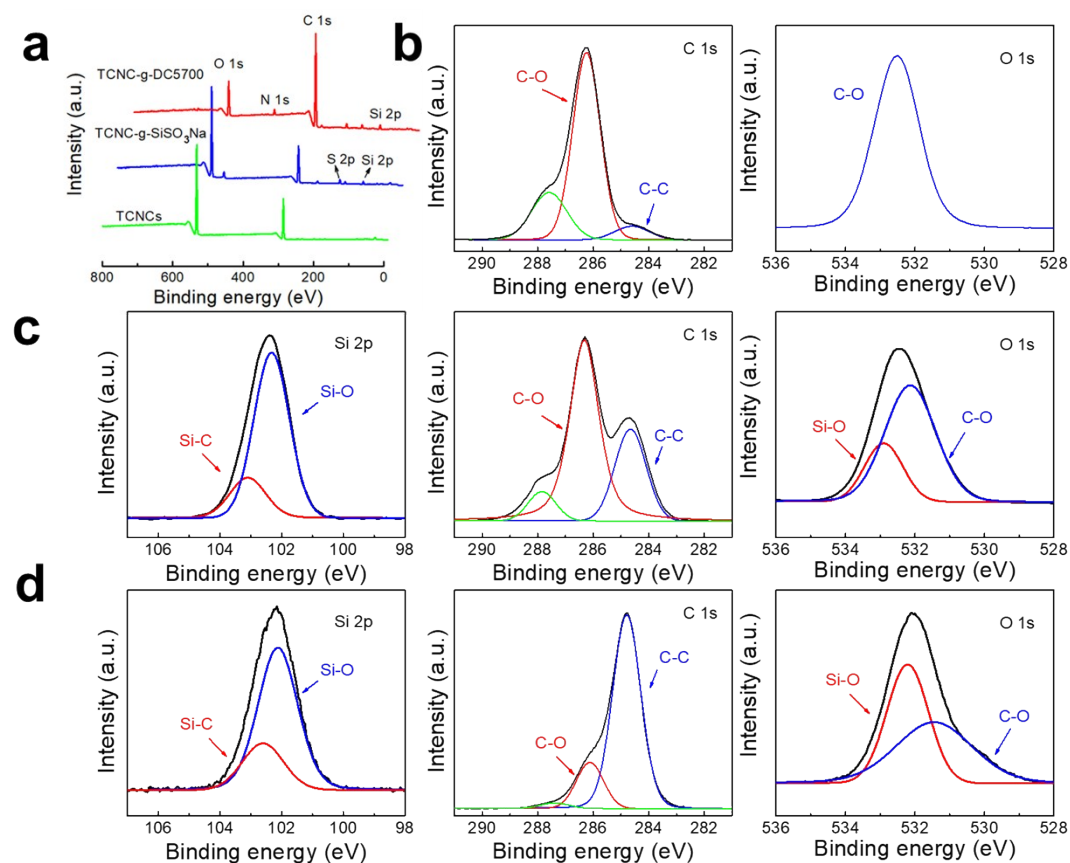
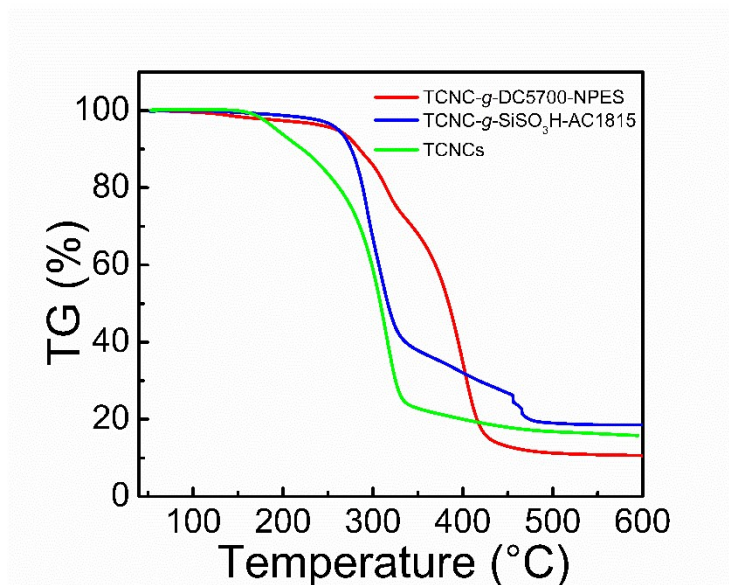


**Fig. S4.** XPS fully scanned spectra of TCNCs, TCNC-g-SiSO<sub>3</sub>Na, and TCNC-g-DC5700 (a); C1s and O1s for TCNCs (b); Si2p, C1s, and O1s for TCNC-g-SiSO<sub>3</sub>Na (c) and TCNC-g-DC5700 (d).



### Thermal gravimetric analysis

**Fig. S5.** Thermal gravimetric curves of TCNCs, TCNC-*g*-SiSO<sub>3</sub>H-AC1815 and TCNC-*g*-DC5700-NPES.

**Table S4.** S and W parameters of TCNCs, TCNC-*g*-SiSO<sub>3</sub>H-AC1815 and TCNC-*g*-DC5700-NPES.

Sample	S	W
TCNCs	0.4858 ± 0.0003	0.01540 ± 0.00005
TCNC- <i>g</i> -SiSO <sub>3</sub> H-AC1815	0.5071 ± 0.0003	0.01303 ± 0.00004
TCNC- <i>g</i> -DC5700-NPES	0.5159 ± 0.0003	0.01159 ± 0.00004

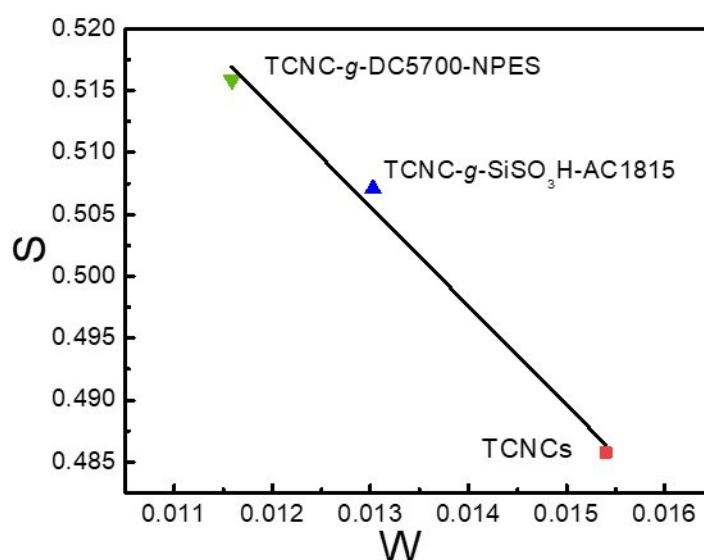


**Fig. S6.** S-W plots of TCNCs, TCNC-g-SiSO<sub>3</sub>H-AC1815 and TCNC-g-DC5700-NPES from Doppler broadening measurement.

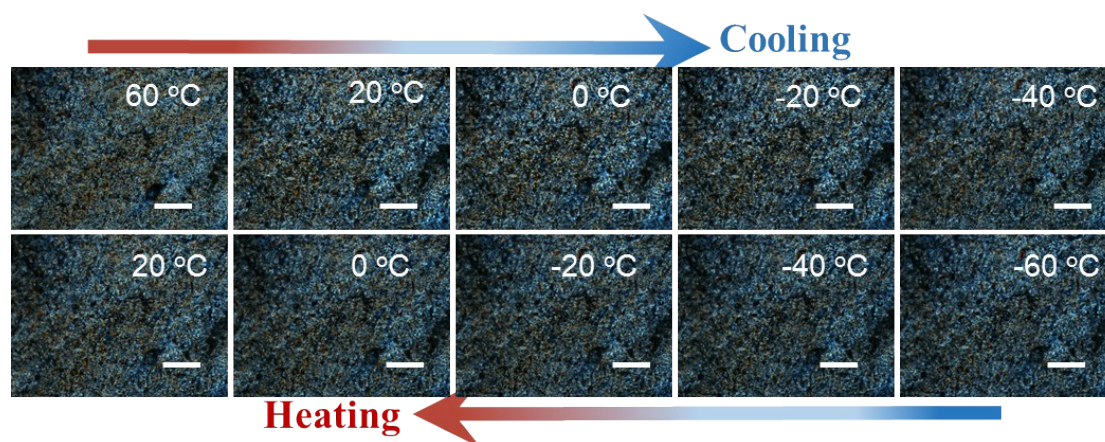


**Fig. S7.** The POM of TCNCs mixed in DC5700-NPES during cooling-heating process (scale bars, 100  $\mu$ m).

## References

- [1] Chen, P.; Nishiyama, Y.; Mazeau, K. Torsional entropy at the origin of the reversible temperature-induced phase transition of cellulose. *Macromolecules* **2011**, *45* (1), 362-368.
- [2] Yoshiharu, N.; Johnson, G. P.; French, A. D.; V Trevor, F.; Paul, L. Neutron crystallography, molecular dynamics, and quantum mechanics studies of the nature of hydrogen bonding in cellulose I $\beta$ . *Biomacromolecules* **2008**, *9* (11), 3133-3140.
- [3] Vanommeslaeghe, K.; MacKerell Jr., A. D. Automation of the CHARMM general force field (CGenFF) I: Bond perception and atom typing. *J. Chem. Inf. Model.* **2012**, *52* (12), 3144-3154.
- [4] Vanommeslaeghe, K.; Raman, E. P.; MacKerell, A. D. Automation of the CHARMM general force field (CGenFF) II: Assignment of bonded parameters and partial atomic charges. *J. Chem. Inf. Model.* **2012**, *52* (12), 3155-3168.

- [5] MacKerell, J. A. D.; Raman, E. P.; Guvench, O. CHARMM additive all-atom force field for glycosidic linkages in carbohydrates involving furanoses. *J. Phys. Chem. B* **2010**, *114* (40), 12981-12994.
- [6] Guvench, O.; Hatcher, E.; Venable, R.; Pastor, R.; MacKerell Jr, A. Additive empirical CHARMM force field for glycosyl linked hexopyranoses. *J. Chem. Theory Comput.* **2009**, *5*, 2353-2370.
- [7] Giovanni, B.; Davide, D.; Michele, P. Canonical sampling through velocity rescaling. *J. Chem. Phys.* **2007**, *126* (1), 2384.
- [8] Berendsen, H. J. C.; Postma, J. P. M.; Gunsteren, W. F. V.; Dinola, A.; Haak, J. R. Molecular dynamics with coupling to an external bath. *J. Chem. Phys.* **1984**, *81* (8), 3684-3690.
- [9] York, D. M.; Darden, T. A.; Pedersen, L. G. The effect of long-range electrostatic interactions in simulations of macromolecular crystals: A comparison of the ewald and truncated list methods. *J. Chem. Phys.* **1993**, *99* (10), 8345-8348.